FROM NEURON TO BRAIN: STATISTICAL PHYSICS OF THE NERVOUS SYSTEM

Paul H.E. Tiesinga
Sloan–Swartz Center for Theoretical Neurobiology and Computional Neurobiology Lab, Salk Institute
10010 N. Torrey Pines Rd, La Jolla, CA 92037, USA
tiesinga@salk.edu

Abstract A common experimental neuroscience protocol is to record the single neuron activity in response to repeated stimulus presentations and analyze how this activity encodes for stimulus properties. Neurons are embedded in a large network and their response properties depend on the dynamical state of the network. I discuss how brain chemicals — neuromodulators — can dynamically change the coherence and frequency content of network activity; how the network coherence affects the neuronal response to current injection and how this can form the neural correlate for an important computation — gain modulation — that the brain performs.

Keywords: neuron, synchronized oscillations, neural coding, gain modulation

1. INTRODUCTION

The brain is a massively interconnected network of neurons that generates spatiotemporally ordered activity on multiple time and length scales. Individual neurons produce all–or–none electric events known as action potentials or spikes. A basic belief in neuroscience is that neurons encode information using action potentials. The fundamental question is how information is encoded, transmitted, processed, and decoded in cortical networks. To make progress, one needs to understand the spiking dynamics of local cortical circuits and how to link their activity to the coherent macroscopic activity detected in electroencephalograms, functional magnetic resonance imaging, and magnetoencephalograms. Biologically informed application of quantitative techniques based on nonlinear dynamics, complex systems theory, statistical physics and information theory are likely to yield important contributions to solving this class of problems.

Developments in Mathematical and Experimental Physics,
Volume B: Statistical Physics and Beyond
Edited by Macias *et al.*, Kluwer Academic/Plenum Publishers, 2003

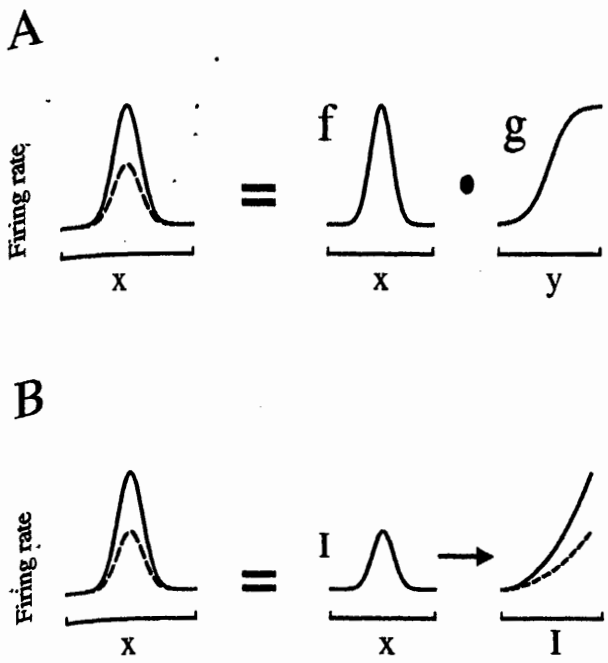

Figure 1. A possible single neuron correlate of gain modulation. (A) Firing rate tuning curves as a function of x for two different values of y (solid and dotted line, respectively). The neural response can be expressed as a product of $f(x)$, the tuning curve for x, and $g(y)$, the gain as a function of y. (B) Stimulus property x causes a tuned current I into the neuron. The resulting firing rate is given by an f–I characteristic that depends on y (the solid and dotted line represent two y values).

In this work I review one particular aspect of local circuit dynamics. A typical neuron receives both input from the network it is embedded in, as well as feedforward input from, for instance, sensory areas. I will discuss how the network state affects the neuron's response to feedforward inputs and, furthermore, what purpose modulation of network activity could potentially subserve.

A common experimental paradigm for studying neural coding is to present a visual stimulus to an animal and record spike trains from single neurons in the appropriate sensory area. A key response quantity is the spike count — the number of spikes emitted by the neuron in a fixed time interval after stimulus presentation. Stimulus characteristics

are then systematically varied in order to assess how they are encoded by the neuron using the spike count.

The mean neuronal firing rate (equal to the spike count normalized for the duration of the measurement) elicited by a stimulus presentation can often be written as a product of stimulus attributes. For instance, the response of neurons in visual cortex to oriented bars is tuned for the orientation x (dotted line in Fig. 1A). When the brightness of the stimulus, y, is increased a similar but rescaled tuning curve is obtained (solid line in Fig. 1A). Hence, the response is a product of the orientation tuning $f(x)$ and the brightness–induced gain modulation $g(y)$ (Fig. 1A).

Gain modulation is a general computational paradigm in the nervous system and it is observed in many cortical areas (reviewed in Refs. [1, 2, 3]). Attention could also gain-modulate orientation tuning curves [4, 5]. Recently, neural correlates of attention were studied experimentally using awake behaving monkeys [6, 7, 8]. Exactly the same two sensory stimuli were presented to the monkey under two conditions: when it had to pay attention to one of the stimuli to perform a task for which it was rewarded; and when it did *not* have to pay attention to that stimulus in order to obtain its reward. During this task, spike trains from one or more neuron(s) in sensory areas were recorded. The feedforward sensory input that the recorded neuron received should be the same under both conditions and any difference in neuronal response between the conditions had to be due to the network state. In one experiment the response of multiple neurons in the secondary somatosensory cortex to tactile stimulation of the finger tips was recorded [6]. When the animal had to pay attention to the tactile stimulus the number of coincident spikes between two simultaneously recorded neurons increased significantly. This effect was independent of changes in firing rate. In the other experiment [7], two visual stimuli were presented to the animal. The first stimulus was in the receptive field of the neuron that was recorded from, whereas the second stimulus was outside the receptive field. The local field potential — an electrical signal that represents the mean activity of a group of neighboring neurons — was recorded simultaneously with the single neuron activity. When the animal focused attention on the stimulus in the receptive field two changes were observed compared with when it payed attention to the stimulus outside this receptive field: (1) the local field potential power in the gamma–frequency band (30-80 Hz) had increased and (2) the coherence of the single neuron discharge with the local field potential had increased. However, the firing rate had not changed significantly.

Both these experiments show that attention can modulate the state of cortical networks, in particular, neural synchrony. Here I explore how

neural synchrony affects the gain of a neuron's response. A key assumption is that stimulus attribute x causes a tuned depolarizing current $I(x)$ into the neuron (Fig. 1B). The resulting firing rate is given by the firing rate-versus current curve (f–I) whose gain depends on stimulus attribute y. Hence, the problem is to determine how the gain of the f–I depends on the amount of synchrony.

The rest of the paper is organized as follows. First, the effect of incoherent network activity on the f–I is studied. Second, the generation of coherent activity by networks is discussed. Then, the effect of coherent network activity on the f–I is investigated. Finally, gain modulation by coherent and incoherent network activity is compared.

2. RESULTS

2.1. GAIN MODULATION BY "BALANCED" SYNAPTIC INPUTS.

The impact of network activity on the response properties of neurons was investigated using model simulations. Full details are given in Ref. [9] (related work is in Refs. [10, 11, 12]). Briefly, a Hodgkin–Huxley–type model neuron was driven by a constant current I and a combination of excitatory and inhibitory shot noises with rates f_e and f_i, respectively. The shot noises represented the network inputs. Each pulse generated a conductance pulse that decayed exponentially in time. The conductance generated a membrane current, I_{syn}, given in Eq. (A.1) of the Appendix. Parameters were chosen to mimick $GABA_A$ inhibitory and AMPA excitatory synaptic inputs [13].

A typical voltage response is shown in Fig. 2A. Network background activity was $f_e = f_i = 750$, but during the time interval indicated by the bar it was reduced to $f_e = f_i = 500$. Action potentials are visible as sharp voltage deflections that cross 0 mV. This computer experiment was repeated 50 times with different shot noise realizations (trials). The spike times were plotted as ticks in a rastergram, each row was a different trial (Fig. 2Ba). The spike time histogram (STH, Fig. 2Bb) was computed by counting the number of spikes in 200 ms bins (normalized to yield spikes per trial per second). During the period of reduced network activity there was an immediate increase in output firing rate.

The amount of injected depolarizing current was varied for different levels of background activity. The output firing rate increased with the level of depolarizing current. Furthermore, the rate of increase — gain — of the resulting f–I depended strongly on network activity: a higher background activity led to a lower gain.

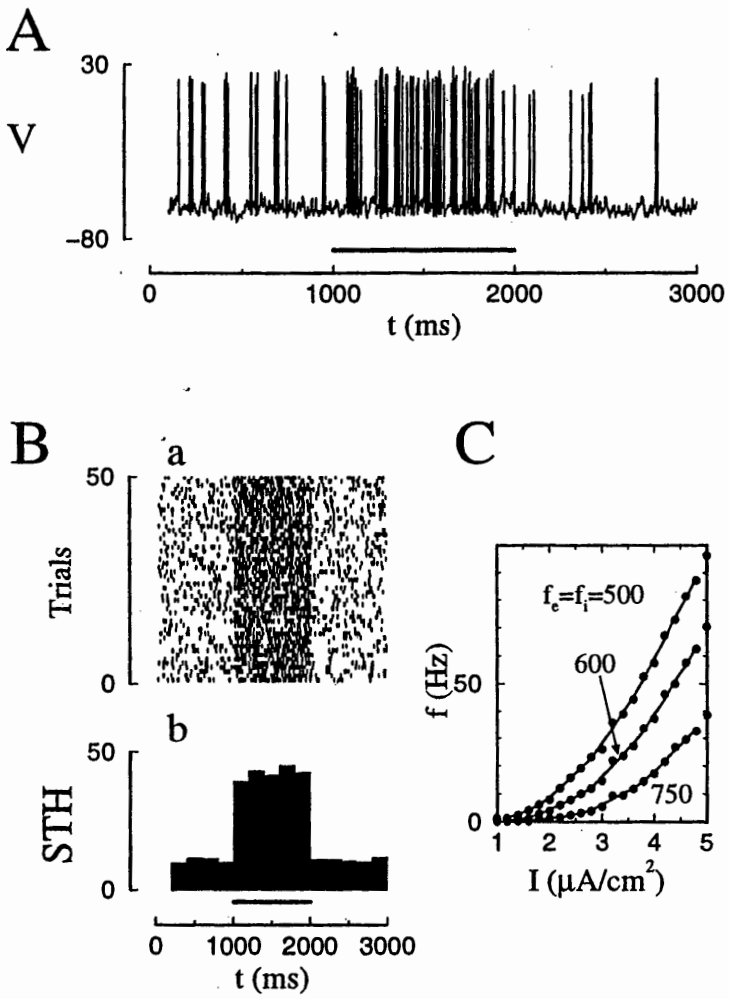

Figure 2. Gain modulation by "balanced" synaptic inputs. The background synaptic activity was reduced from $f_i = f_e = 750$ Hz to 500 Hz between $t = 1000$ ms and 2000 ms (indicated by the bar in A and Bb). (A) Voltage (in mV) versus time during the first trial and (B) (a) rastergram and (b) spike time histogram (STH) for 50 trials is shown. (C) The mean firing rate as a function of injected current I for different levels of background synaptic activity as is indicated in the graph. Averages were obtained over 20 s.

What is the significance of this result? The depolarizing current is the feedforward signal coming from sensory areas. The neural response to the signal, I, thus depends on the state of the network the neuron is embedded in. The firing rate recorded *in vivo* therefore does not uniquely represent a particular input signal. However, as pointed out by Chance & Abbott [14], this mechanism can form the neural substrate for gain modulation.

The type of network activity the neuron received is sometimes called balanced [11, 15, 16, 17] (or fluctuation–dominated [9]). The idea is that the *average* effect of the excitatory and inhibitory inputs is approximately the same but opposite in sign, that is, balanced. The mean drive remains below spiking threshold and spiking is caused by fluctuations. The fluctuations can be varied by increasing the network activity in such a way that it remains balanced. For incoherent inputs, Poisson spike trains with a time–independent rate, there are only two parameters that can be varied: the rates f_i and f_e (under the assumption that the unitary amplitude and decay time constant of the pulses remain constant). However, the synaptic drive yields a mean conductance, Eq. (A.2) and a mean current, Eq. (A.3) (see Appendix). Only one of these can be held constant. Hence, one can have either have a balanced "current" [9] or "conductance" drive [14].

2.2. COHERENT ACTIVITY OF NEURONAL NETWORKS

Neuronal networks spontaneously generate synchronized oscillations in different frequency bands. For instance, the human electroencephalogram (EEG) contains multiple synchronous rhythms that reflect spatially and temporally ordered activity [18, 19]. Delta rhythms (0.5 – 2 Hz) are involved in signal detection and decision making [20]; theta oscillations (4 – 12 Hz) are related to cognitive processing [21]; and gamma oscillations (30 – 80 Hz) can be found in a variety of structures under different behavioral conditions [18, 22, 23]. The neural mechanisms for these correlated changes in EEG frequency content are unknown, but they are likely to involve a class of brain chemicals known as neuromodulators [24, 25, 26]. For instance, in vivo studies in cats show that the level of the neuromodulator acetylcholine in the cortex and hippocampus (a brain area involved in memory processes) is reduced during delta oscillations, and can be up to four times higher during theta activity [27].

The in vitro hippocampal preparation has provided a simplified framework, which allows the mechanisms underlying theta, delta and gamma

rhythms, and the transitions between the rhythms to be studied. Activation of the CA3 region in hippocampus, using the agonist carbachol (a substance with similar effects as acetylcholine), results in synchronous population activity in the delta [28, 29], theta [30, 29, 31, 32, 33], and gamma [29, 34] bands. The carbachol concentration in the slice determines which of the three oscillations will occur or predominate [29].

The biophysical effects of carbachol have been studied extensively. Each neuron has a diverse set of voltage–gated ionic channels in its membrane. The density and types of channels determines a neuron's dynamics. Carbachol blocks several channels in a concentration dependent manner [35, 36]. This makes neurons more excitable, unmasking subthreshold membrane potential oscillations in the theta–frequency range [37, 29]. In addition, carbachol reduces the average strength of excitatory synaptic coupling between neurons [38, 39, 40]. Therefore, carbachol changes the intrinsic neuronal dynamics and the network dynamics, which has made it difficult to dissect these two contributions solely by experimental methods. Recently my colleagues and I determined using model simulations under what conditions, and by what mechanisms, the hippocampal area CA3 can support the CCH-δ, CCH-θ, and CCH-γ oscillations [41]. In particular, we investigated how carbachol induced transitions between these states in a concentration dependent manner. These results show that even a single neuromodulator can exert a powerful control on the coherence and frequency content of network activity. I will now focus on gamma oscillations in networks of interneurons [42, 43, 44], since, as mentioned in the introduction, gamma–band activity is thought to be important for attention. Attention was associated with increased synchrony of the modulatory input but the mean firing rate did not significantly increase. I explored under what conditions synchrony of a coupled network could be varied independently of mean firing rate. The result for an all–to–all coupled inhibitory network is shown in Fig. 3A. The neurons in this network are connected by inhibitory synapses. Hence, when a particular neuron becomes more active, it *reduces* the activity of the neurons it is connected to.

A depolarizing current pulse of 500 ms duration was applied to all neurons at $t = 1000\ ms$. The pulse represented the effects of, for instance, the release of acetylcholine. Initially, the network was asynchronous, the spike time histogram did not have any peaks and the mean firing rate in the network was approximately 8 Hz. It took approximately 300 ms for the network to synchronize, at that time sharp peaks appeared in the spike time histogram. The firing rate only increased marginally to 9 Hz. It is, of course, not known whether the effects of attention can be represented by a depolarizing current or whether the attention–

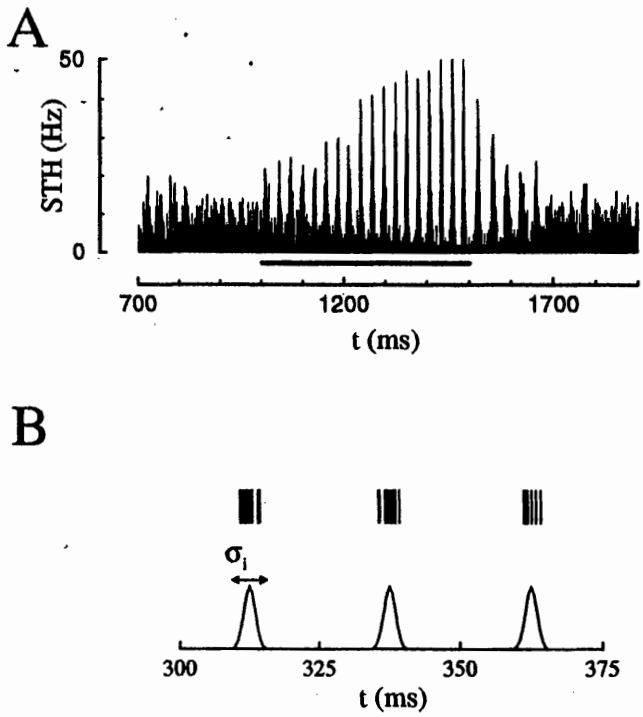

Figure 3. (A) The inhibitory network synchronized in response to a brief depolarizing current pulse (indicated by the bar) to 25% of the neurons. (B) Coherent network discharge was modelled as (top) an inhomogeneous Poisson spike train with (bottom) a spike time probability density consisting of a periodic sequence of Gaussians of width σ_i. The probability density was normalized so that the mean rate was f_i.

related networks have an all–to–all architecture. However, the results are a proof of principle that it is possible to modulate neural synchrony independently of mean network activity.

Synchronous network activity can be modelled in a less computationally intensive way as is shown in Fig. 3B. The network spike time histogram consisted of a sequence of Gaussian functions with width σ_i. Input spike times were generated as a Poisson process from the STH [44, 45, 46]. The degree of neural synchrony was correlated with the width, σ_i, of peaks in the STH. Low values of σ_i corresponded to high synchrony and high values of σ_i corresponded to low synchrony. As before, each spike generated unitary conductance pulses of amplitude Δs_i and a decay time τ_i (see Appendix for details).

2.3. GAIN MODULATION BY NEURAL SYNCHRONY.

The neuron received two types of inputs, a feedforward projection that was modelled as a constant depolarizing current and a modulatory input representing, for instance, the effects of attention. The modulatory input was modelled as an synchronous inhibitory synaptic drive. The effects of attention were modelled by reducing σ_i from 8 ms to 2 ms during a 500 ms long pulse (indicated by the bar in Fig. 4A). Without attention the neuron did not fire, but as soon as input synchrony was increased it started firing. The attentional effect was reversible: as soon as the synchrony was reduced to its original value the neuron stopped firing.

There were two sources of variability in the synaptic inputs: jitter in the position of the Gaussian peaks in the spike time density for the Poisson process (Fig. 3B, bottom) and the particular realization of the Poisson spike train given a particular spike time density (Fig. 3B, top). To assess the effect of the variability on the neuronal response the simulation was repeated 500 times with independent realizations (Fig. 4B). The transient increase of synchrony reliably led to an increased firing rate (Fig. 4Ba). The resulting spike time histogram during the period of increased input synchrony was flat. This means that although there were signs of output periodicity during a given trial (Fig. 4A), the timing across different trials was not maintained. Hence, in this case, the precise timing of spikes on a given trial does not carry stimulus information. Note, however, that the spike time histogram obtained from an *ensemble* of neurons receiving the same synaptic drive will be peaked.

The firing rate versus current characteristic was determined for three values of the synchrony parameter σ_i (Fig. 4C). As before, the firing rate increased with the level of depolarizing current. However, the rate of increase was higher for more synchronous inputs, that is, lower values of σ_i. At first instance, this may seem counterintuitive: A more synchronous inhibitory drive results in a more effective inhibition yet it yields a higher firing rate. Just after the arrival of the input pulses the synaptic conductance reaches its highest value. Over a time period on the order of the synaptic decay constant, τ_i, the conductance decays to its lowest value. The synaptic drive thus has two components, the phasic component, quantified as the difference between maximum and minimum conductance value, and the tonic component equal to the minimum conductance value. The neuron can only fire when inhibition has sufficiently decayed. Whether or not a neuron can fire is determined by the value of the tonic component. Higher synchrony — lower

σ_i — leads to a higher phasic and a lower tonic component. The parameters of the simulations were chosen such that for an asynchronous drive, $\sigma_i = 10$ ms, the tonic component was so large that the neuron did not spike, whereas for a synchronous drive it could fire. An alternative viewpoint is as follows. The neuron can be approximately considered as a threshold device. The parameters were tuned so that the neuron was below threshold and could only fire when voltage fluctuations drove it across threshold. A higher phasic component leads to larger voltage fluctuations, hence a higher firing rate. This hypothesis was confirmed by comparing the variance of voltage fluctuations with the firing rate when varying σ_i (results not shown).

Gain modulation with synchrony is only possible when the firing rate was actually modulated by σ_i. The conditions under which this occurred were determined. Two parameters were important: the frequency, f_{net}, of the synchronous inhibitory barrages (equal to the inverse of the distance between consecutive Gaussian peaks in Fig. 3B, the default value was $f_{net} = 40$ Hz) and the synaptic decay time constant τ_i. A measure for the maximal gain is the firing rate for $\sigma_i = 1$ divided by the firing rate for $\sigma_i = 10$. This ratio had an optimal value as a function of f_{net}. For $\tau_i = 10$ ms — the default value used here to model $GABA_A$ synaptic inputs — the position of the optimum was in the gamma frequency range. The position of the optimum depended on τ_i: it shifted to higher frequencies as τ_i was decreased. Full details will be given elsewhere [47, 48]

3. DISCUSSION

Gain modulation is an important computational mechanism for representing two or more stimulus attributes in a neuron's firing rate. Here two possible mechanisms for implementing gain modulation were presented. They work by modulating the response to feedforward sensory inputs that were modelled as a depolarizing current. The mechanisms were studied by calculating the firing rate versus current characteristic (f–I). The first mechanism is based on balanced synaptic inputs and was proposed by Chance & Abbott [14]. The gain of the f–I was reduced by proportionally increasing both the excitatory and inhibitory activity. An alternative mechanism proposed here is based on modulating synchrony. The gain of the f–I increased with synchrony. I also showed using model simulations that network synchrony could easily be manipulated using neuromodulators. The gain modulation corresponds to a multiplicative rescaling of the $f - -I$. This is sometimes hard to assess from the $f - I$ curves themselves. However, the sensitivity of the

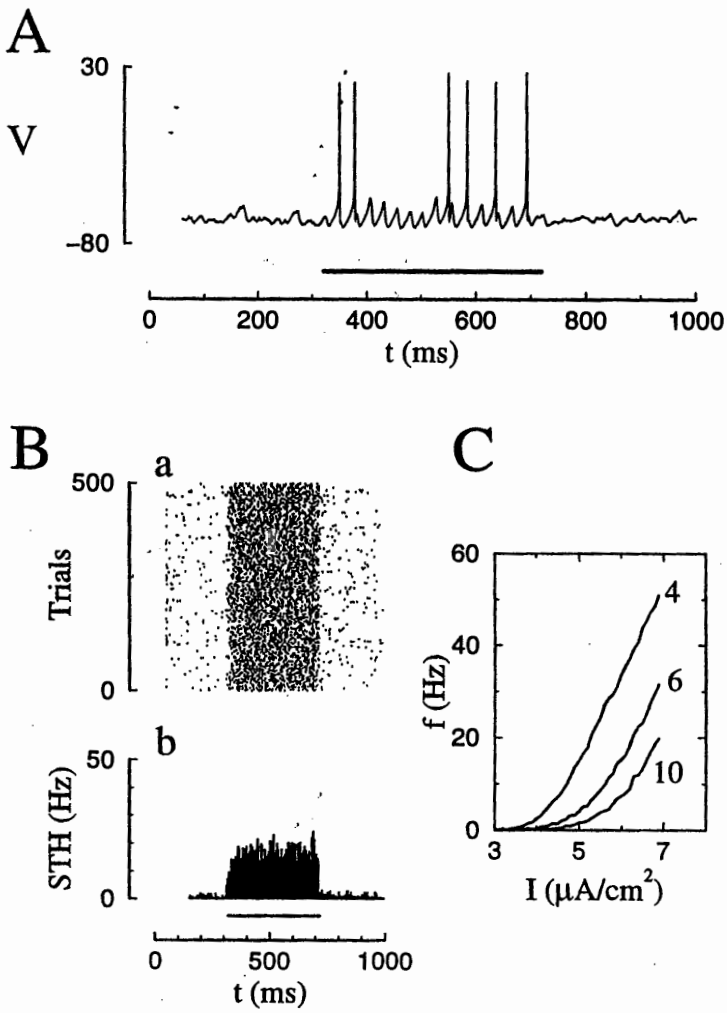

Figure 4. Gain modulation by synchrony. The synchony was increased between $t = 270$ ms and 520 ms by decreasing σ_i from 8 ms to 2 ms. (A) Voltage (in mV) versus time during one trial, (B) (a) rastergram and (b) STH for 500 trials. (C) f–I characteristic for different values of σ_i, as is labeled in the graph.

firing rate to current changes, df/dI, plotted versus I or f yields a better test of multiplicative rescaling (L.F. Abbott, personal communication).

The underlying biophysics was similar for both mechanisms: it uses the fact that neurons are threshold devices. The membrane voltage of the neuron is on average subthreshold and spikes are induced by fluctuations. The gain is adjusted by changing the variance of the fluctuations

while the neuron remains subthreshold. For balanced synaptic inputs, the fluctuations are modulated by covarying excitatory and inhibitory input rates at a fixed ratio. Increasing input rates changes both the mean synaptic conductance as well as the mean current. The ratio between f_i and f_e can be chosen to keep either the mean current or mean conductance constant, but not both at the same time. Hence, the distance to threshold may also change during manipulations of the balanced synaptic input. For gain modulation with synchrony, the mean conductance always remained the same, and the mean driving current changed very little for the parameters considered here (results not shown). Hence, synchrony works by directly affecting voltage fluctuations, without changing the means of the drive.

The dynamics of single neurons is often studied in the *in vitro* preparation. A slice of cortical tissue is kept "alive" in a solution resembling corticospinal fluid. A depolarizing current is injected into the neuron using an intracellular electrode and the voltage response is recorded. The firing rate of the neuron — number of action potentials per second — is then determined as a function of the amplitude, I, of the injected current. *In vitro* neurons do not receive the synaptic drive due to network activity. Recently, experimental techniques have been developed to study "*in vivo*" dynamics of neurons using the *in vitro* slice preparation. The network activity is injected into the neuron using so–called dynamic clamp [49]. Some of the modelling results reported here were confirmed using this technique [47]. Hence, both mechanisms could potentially subserve gain modulation in cortical tissue. Recent experiments have shown that modulating network coherence is an important component of attention, but a conclusive *in vivo* experiment explicitly linking attentional gain modulation to synchrony is still lacking. Furthermore, an important theoretical issue is how to generalize gain modulation of one neuron to that of a interacting network of neurons.

Acknowledgments

The results reported in this proceedings are based on work done in collaboration with Jean–Marc Fellous, Jorge V. José, Emilio Salinas and Terry Sejnowski. I thank the Sloan–Swartz Center for Theoretical Neurobiology for financial support. Part of the calculation was performed at Northeastern University High Performance computer center. I thank the organizers of the "1st Mexican Meeting on Mathematical and Experimental Physics" for their hospitality during my visit to Mexico city.

Appendix

The synaptic drive injected into the model neuron was a sum of inhibitory and excitatory conductances,

$$I_{syn} = g_e s_e(t)(V - E_e) + g_i s_i(t)(V - E_i). \tag{A.1}$$

Where the conductance was $g_e = g_i = 1.0\,mS/cm^2$, and the reversal potentials were $E_e = 0\ mV$ and $E_i = -75\ mV$, for the excitatory (AMPA) and inhibitory ($GABA_A$) synapses, respectively. Unitary excitatory (inhibitory) postsynaptic potentials were modelled as quantal conductance increases, $\Delta s_e = 0.02$ ($\Delta s_i = 0.05$), in the synaptic kinetic variable $s_e(t)$ ($s_i(t)$). The conductance pulses in $s_e(t)$ and $s_i(t)$ decayed exponentially in time with a time constant $\tau_e = 2$ ms ($\tau_i = 10$ ms). The postsynaptic potentials were independent and formed either a homogeneous or an inhomogeneous (see Fig. 3B) Poisson process with average rates f_e and f_i, respectively.

The mean of the total synaptic conductance was,

$$\langle g_{syn} \rangle = g_e \langle s_e \rangle + g_i \langle s_i \rangle, \tag{A.2}$$

and the mean of the driving current I_{syn} was

$$\langle I_{syn} \rangle = \beta_e \langle s_e \rangle + \beta_i \langle s_i \rangle, \tag{A.3}$$

with $\beta_e = g_e(E_e - V_{rest})$, and $\langle s_e \rangle = \tau_e f_e \Delta s_e$ (with similar expressions for the inhibitory part); V_{rest} was the resting membrane potential. The last expression is only valid for weak synaptic drives, unlike the ones used here, see Ref. [9] for details.

References

[1] E. Salinas and P. Thier, *Neuron* **27** (2001) 15.

[2] E. Salinas and T. Sejnowski, *Nat Rev Neurosci* **2** (2001) 539.

[3] E. Salinas and T. Sejnowski, *Neuroscientist* **7** (2001) 430.

[4] C. McAdams and J. Maunsell, *J. Neurosci.* **19** (1999) 431.

[5] S. Treue and J. Martinez Trujillo, *Nature* **399** (1999) 575.

[6] P. Steinmetz *et al.*, *Nature* **404** (2000) 187.

[7] P. Fries, J. Reynolds, A. Rorie, and R. Desimone, *Science* **291** (2001) 1560.

[8] S. Treue, *Trends Neurosci.* **24** (2001) 295.

[9] P. Tiesinga, J. José, and T. Sejnowski, *Phys. Rev.* **E62** (2000) 8413.

[10] D. Pare and A. Destexhe, *J. Neurophysiol.* **81** (1999) 1531.

[11] E. Salinas and T. Sejnowski, *J. Neurosci.* **20** (2000) 6193.

[12] A. Destexhe, M. Rudolph, J.-M. Fellous, and T. Sejnowski, *Neuroscience* **107** (2001) 13.

[13] G. Shepherd, *The synaptic organization of the brain* (Oxford University Press, New York, 1998).

[14] F. Chance and L. Abbott, *Soc. Neurosci. Abstr.* **26** (2000) 1064.

[15] M. Shadlen and W. Newsome, *J. Neurosci.* **18** (1998) 3870.

[16] S. Song, K. Miller, and L. Abbott, *Nat. Neurosci.* **3** (2000) 919.

[17] A. Burkitt, *Biol. Cybern.* **85** (2001) 247.

[18] E. Basar, C. Basar–Eroglu, S. Karakas, and M. Schurmann, *Neurosci. Lett.* **259** (1999) 165.

[19] A. Glass and R. Riding, *Biol. Psychol.* **51** (1999) 23.
[20] C. Basar–Eroglu, E. Basar, T: Demiralp, and M. Schurmann, *Int. J. Psychophysiol.* **13** (1992) 161.
[21] O. Vinogradova, *Prog. Neurobiol.* **45** (1995) 523.
[22] R. Ritz and T. Sejnowski, *Curr. Opin. Neurobiol.* **7** (1997) 536.
[23] W. Singer and C. Gray, *Annu. Rev. Neurosci.* **18** (1995) 555.
[24] D. McCormick, *Prog. Neurobiol.* **39** (1992) 337.
[25] M. Stewart and S. Fox, *Trends Neurosci.* **13** (1990) 163.
[26] L. Leung, *Neurosci. Biobehav. Rev.* **22** (1998) 275.
[27] F. Marrosu *et al.*, *Eur. J. Neurosci.* **7** (1995) 358.
[28] J. Boguszewicz, B. Skrajny, J. Kohli, and S. Roth, *Can. J. Physiol. Pharmacol.* **74** (1996) 1322.
[29] J.-M. Fellous and T. Sejnowski, *Hippocampus* **10** (2000) 187.
[30] B. Bland, L. Colom, J. Konopacki, and S. Roth, *Brain Res.* **447** (1988) 364.
[31] J. Konopacki, M. MacIver, B. Bland, and S. Roth, *Brain Res.* **405** (1987) 196.
[32] B. MacVicar and F. Tse, *J. Physiol. (Lond)* **417** (1989) 197.
[33] J. Williams and J. Kauer, *J. Neurophysiol.* **78** (1997) 2631.
[34] A. Fisahn, F. Pike, E. Buhl, and O. Paulsen, *Nature* **394** (1998) 186.
[35] D. Madison, B. Lancaster, and R. Nicoll, *J. Neurosci.* **7** (1987) 733.
[36] D. McCormick, *Trends Neurosci.* **12** (1989) 215.
[37] L. Leung and C. Yim, *Brain Res.* **553** (1991) 261.
[38] M. Hasselmo, *Behav. Brain Res.* **67** (1995) 1.
[39] M. Hasselmo, E. Schnell, and E. Barkai, *J. Neurosci.* **15** (1995) 5249.
[40] M. Patil and M. Hasselmo, *J. Neurophysiol.* **81** (1999) 2103.
[41] P. Tiesinga, J.-M. Fellous, J. José, and T. Sejnowski, *Hippocampus* **11** (2001) 251.
[42] X.-J. Wang and G. Buzsáki, *J. Neurosci.* **16** (1996) 6402.
[43] J. White *et al.*, *J. Comput. Neurosci.* **5** (1998) 5.
[44] P. Tiesinga and J. José, *Network* **11** (2000) 1.
[45] P. Tiesinga, J.-M. Fellous, J. José, and T. Sejnowski, *Network* **13** (2002) 41.
[46] P. Tiesinga, J.-M. Fellous, J. José, and T. Sejnowski, *Neurocomputing* **38-40** (2001) 397.
[47] J. José *et al.*, *Soc. Neurosci. Abstr.* 722.11 (2001).
[48] P. Tiesinga *et al.*, in preparation (2002).
[49] A. Sharp, M. O'Neil, L. Abbott, E. Marder, *Trends Neurosci.* **16** (1993) 389.